

EUROFEL-Report-2006-DS2-022

EUROPEAN FEL Design Study



Deliverable N°: D 2.8

Deliverable Title: Modelling and validation of bunch compressor schemes at ERLP and FERMI

Task: DS-2

Authors: S. di Mitri et al.

Contract N°: 011935

**Project funded by the European Community
under the “Structuring the European Research Area” Specific Programme
Research Infrastructures action**

Design of magnetic compressors for FERMI@elettra

S. Di Mitri

*Sincrotrone Trieste S.C.p.A., Strada Statale 14 - km 163,5 in AREA Science Park, 34012
Basovizza, Trieste, ITALY*

**Project funded by the European Community
under the “Structuring the European Research Area” Specific Programme
Research Infrastructures action**

1. Introduction

This note addresses some technical aspects of the two magnetic chicanes used for the bunch compression in the Fermi Linac. The range of operation of the parameters involved in such a study has been evaluated according to the following assumptions:

- Double compression scheme (considerations about the single compression scheme are in the Appendix).
- Symmetric magnetic chicanes made of four identical rectangular dipoles.
- Linear compression approximation (beam dynamics at 1st order in the particle coordinates).
- Golden simulations for the Short, Medium and Long bunch cases have been taken as reference cases, together with some other related studies.

As for the analytical description of the bunch length compression, the following approximations have been applied to the beam acceleration:

- Cos-like accelerating voltage.
- Negligible acceleration in the Gun.
- Injector accelerating on crest.
- High harmonic cavity set with 18 MeV peak voltage and on crest in decelerating mode.

Table 1 lists some global parameters concerning the beam compression. Table 2 and Table 3 show the detailed parameters regarding the compression in BC1 and BC2, respectively.

Table 1: Global beam parameters

Bunch type	Charge [nC]	Comp. factor	Δt_i FW [ps]	Δt_f FW [ps]	$I_{core,i}$ [A]	$I_{core,f}$ [A]
SHORT	0.33	27	4.5	0.17	75	1800
MEDIUM	0.8	10	9	0.9	90	850
LONG	1.0	7.5	11	1.5	90	600

Table 2: BC1 compression parameters

Bunch type	L1 phase [rad]	θ_b [rad]	R_{56} [mm]	Comp. Factor
SHORT	-36	0.0750	-31.9	17.9
MEDIUM	-36	0.0703	-28.0	5.8
LONG	-25	0.0703	-28.0	2.2

Table 3: BC2 compression parameters

Bunch type	L2 phase [rad]	L3 phase [rad]	θ_b [rad]	R_{56} [mm]	Comp. Factor
SHORT	-10	-10	0.0582	-19.2	1.5
MEDIUM	-20	-20	0.0535	-16.2	1.7
LONG	-18	-18	0.0775	-34.0	3.5

2. Compression in BC1

2.1 Acceleration

The acceleration in the upstream L1 and in the 4th harmonic cavity is described by mean of the following definitions:

$$\lambda_{\text{RF}} := 0.1\text{m} \qquad k := 2 \frac{\pi}{\lambda_{\text{RF}}} \text{ float,5} \rightarrow \frac{62.832}{\text{m}}$$

The peak voltages of the Injector, of L1 and of the harmonic cavity are:

$$U_0 = 100 \text{ MeV} \qquad U_1 = 188 \text{ MeV} \qquad U_4 = 18 \text{ MeV}$$

Thus, the average beam energy at BC1 is:

$$E_f(\phi_1) := U_0 + U_1 \cdot \cos(\phi_1) + U_4 \cos(\phi_4)$$

A first choice of the range of operation for the L1 phase has been chosen:

$$-42 \text{ deg} < \phi_1 < -20 \text{ deg}$$

Figure 1 illustrates the average energy at BC1 as function of the L1 phase in the chosen range.

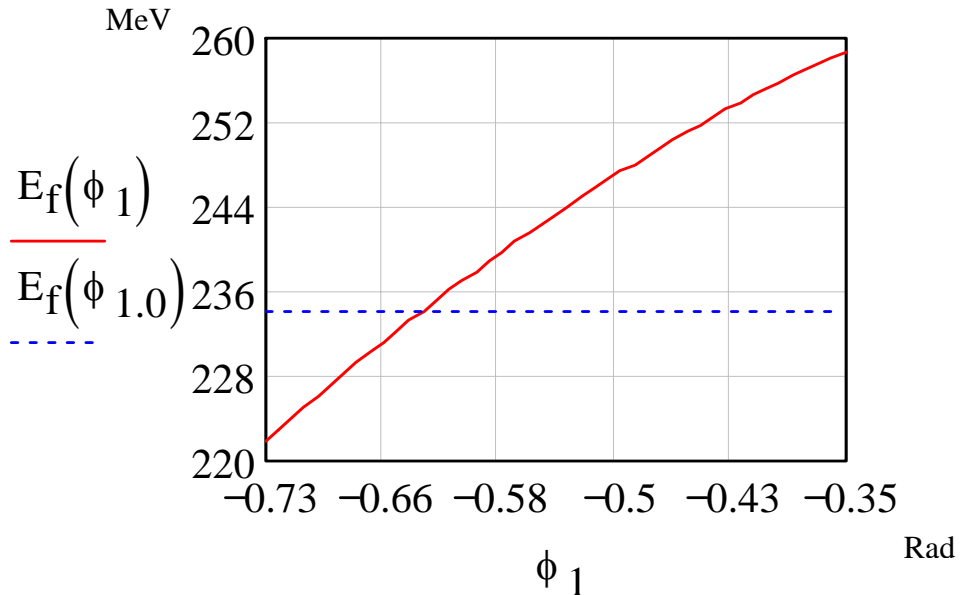


Figure 1: average beam energy at BC1 as function of the L1 phase (red line). The dashed line shows the nominal energy for the medium bunch case.

Absolute spread in momentum is assumed to be constant at BC1 over the L1 phase variation in the range mentioned above; in particular, it has been taken corresponding to the maximum relative energy spread over all the three scenarios, that is 2.5% at 234 MeV, giving $\Delta p = 6 \text{ MeV}$. RMS relative energy spread is plotted as function of the L1 phase in Figure 2.

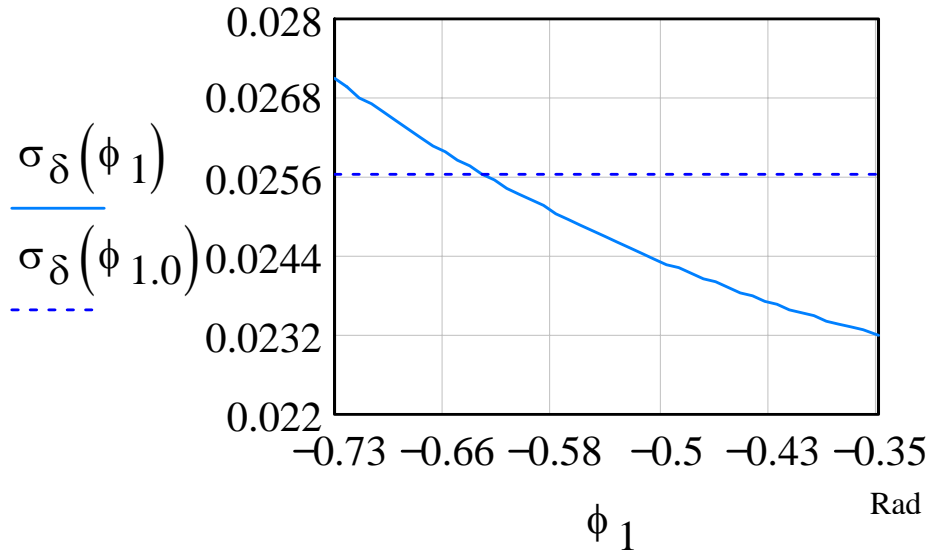


Figure 2: RMS relative energy spread at BC1 as function of the L1 phase (red line). The dashed line is the nominal value for the medium bunch case.

2.2 Compression factor

The linear compression factor in a magnetic chicane is defined as function of the linear energy chirp h and of the R_{56} term:

$$C(\phi_1, \theta) := \frac{1}{1 + h(\phi_1) \cdot R_{56}(\theta)}$$

where:

$$h(\phi_1) := \frac{-k \cdot U_1 \cdot \sin(\phi_1) + \frac{1}{4} \cdot k \cdot (U_0 + U_1 \cdot \cos(\phi_1)) \cdot \tan(\phi_4)}{E_f(\phi_1)}$$

$$R_{56}(\theta) := -2\theta^2 \left(L + \frac{2}{3} \right)$$

The R_{56} term is determined by the chicane geometry. Both BC1 and BC2 are made by four dipoles with magnetic length $l = 0.5$ m and by the drift length between 1st and 2nd, 3rd and 4th dipoles $L = 2.5$ m (see, Figure 3). Figure 4 shows R_{56} as function of the bending angle in the range $0.03 \text{ rad} < \theta_b < 0.10 \text{ rad}$.

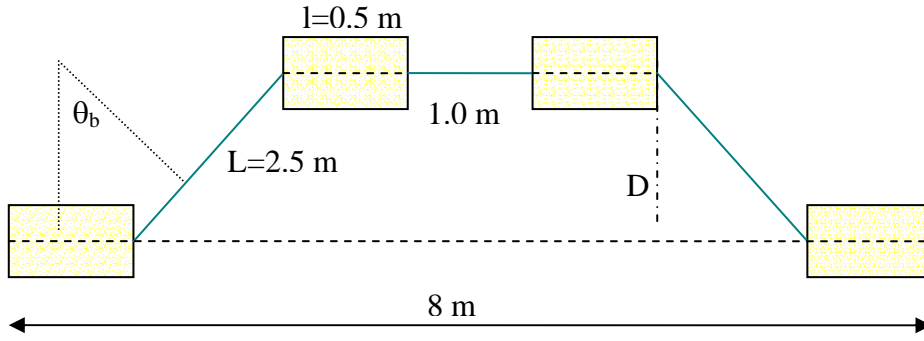


Figure 3: schematic of the symmetric chicane composed by four rectangular dipoles. Lengths refer to both BC1 and BC2.

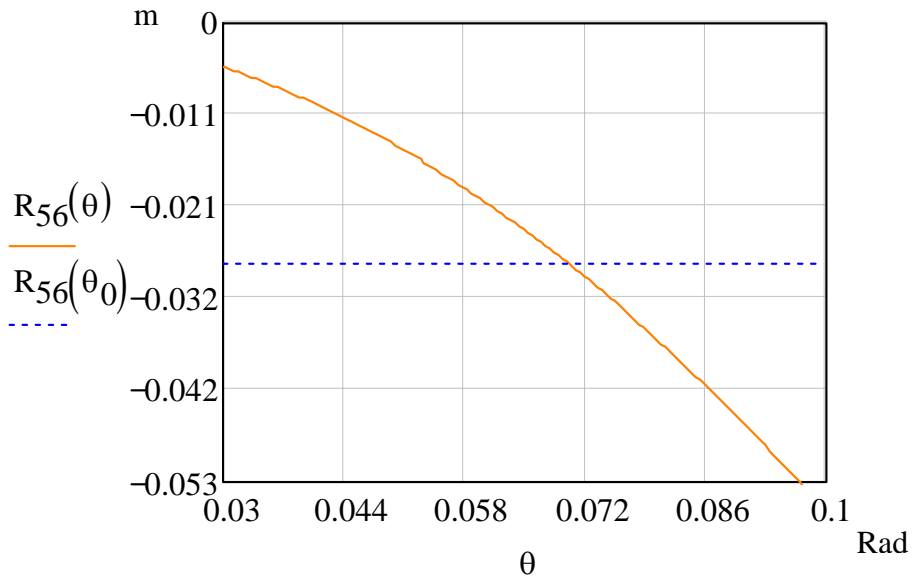


Figure 4: R_{56} term of the linear transport matrix of BC1 as function of the bending angle θ_b (solid line). The dashed line is the nominal value for the medium bunch case.

The linear compression factor has been evaluated as function of the L1 phase and for several discrete values of the bending angle in the chicane, reported in Table 4:

Table 4: bending angle in BC1

	θ_0	θ_1	θ_2	θ_3	θ_4	θ_5	θ_6	θ_7
Bending angle [rad]	0.0703	0.03	0.04	0.05	0.06	0.073	0.08	0.09

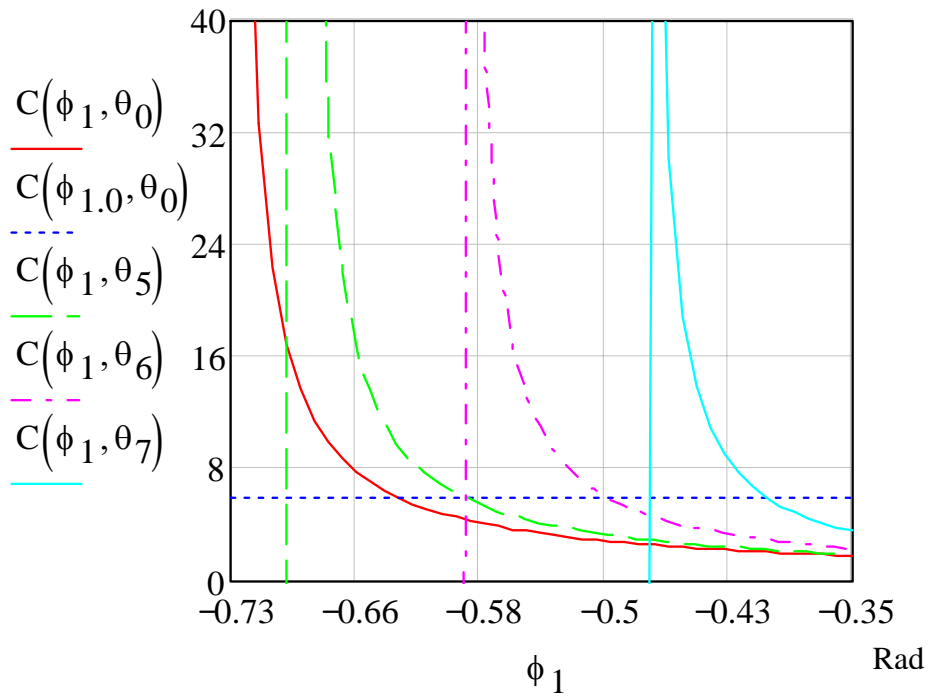
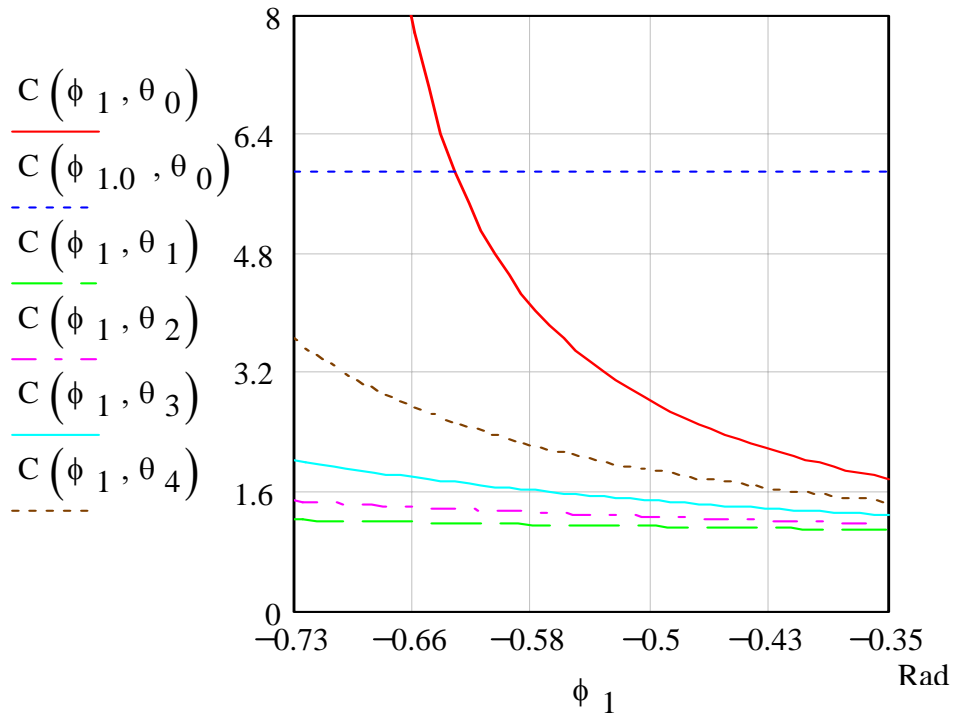


Figure 5 (upper) and Figure 6 (lower): compression factor in BC1 as function of the upstream L1 phase. Each curve refers to a parametric value of the bending angle, as listed in Table 4. The red line is the compression factor for the nominal bending angle of the medium bunch case. The blue dashed line is the compression factor for the both the nominal bending angle and L1 phase for the medium bunch case. Figure 6 shows curves which reaches the maximum compression.

2.3 Specifications for the nominal compression parameters

Each of the three scenarios for the final bunch addresses a different range of parameters variation in each of the two chicanes. Table 5 lists the range of operation for the L1 phase and the bending angle in BC1 for all the three scenarios. A safety margin of $\pm 20\%$ has been applied to the nominal compression factor, which translates into margins for the two variables:

Table 5: nominal ranges of operation for the bunch compression in BC1

	L1 Phase [deg]	Bending angle [rad]
SHORT	$-36.27 < \phi_1 < -35.51$	$0.07441 < \theta_b < 0.07533$
MEDIUM	$-37.5 < \phi_1 < -34.5$	$0.0686 < \theta_b < 0.0716$
LONG	$-29.7 < \phi_1 < -22.7$	$0.0668 < \theta_b < 0.0772$

The corresponding variation of the average beam energy and of the relative energy spread at BC1 are quite small. As a conclusion, the ranges of operation requested from the nominal design for all the three scenarios and taking into account a $\pm 20\%$ variation of the compression factor at BC1 are:

$$-37.5 \text{ deg} < \phi_1 < -22.7 \text{ deg}$$

$$0.0668 \text{ rad} < \theta_b < 0.0772 \text{ rad}$$

These ranges allow a compression factor at BC1 within the range:

$$2.0 < \text{C.F.} < 21.6.$$

2.4 Specifications for the exploratory compression parameters

Figure 6 (see, the violet dashed curve) shows that it is possible to reach a very high compression factor just in the only BC1 with the L1 phase within the range already defined by:

$$-42 \text{ deg} < \phi_1 < -20 \text{ deg}$$

and with a maximum bending angle (including margins):

$$\theta_b < 0.085 \text{ rad}$$

In such a way, a total compression factor of about 100 seems to be obtainable in a double compression scheme. On the other hand, a minimum compression may be achieved by mean of the on-crest acceleration in the L1. This consideration suggests a minimum bending angle (including margins):

$$\theta_b > 0.055 \text{ rad}$$

Notice that the range of operation chosen for the L1 phase implies a maximum reduction of the nominal energy at BC1 by 12 MeV (about 5%) and a maximum RMS relative energy spread of about 2.7% (see, Figure 1 and Figure 2, respectively).

2.5 Transverse displacement of the beam centroid and vacuum chamber

The location of the maximum dispersion and maximum transverse displacement, which are obviously defined in the bending plane, is in the drift between the 2nd and the 3rd dipole. According to the previous ranges of operation, the maximum transverse displacement of the reference trajectory w.r.t. the straight path and the maximum horizontal dispersion may be calculated as follow:

$$D(\theta) := 2 \cdot l \cdot \frac{1 - \cos(\theta)}{\sin(\theta)} + L \cdot \tan(\theta)$$

$$\eta(\theta) := 2 \cdot l \cdot \frac{1 - \cos(\theta)}{\tan(\theta)} + L \cdot (\tan(\theta) + \tan(\theta)^2)$$

They are plotted in Figure 7 as function of the bending angle in BC1.

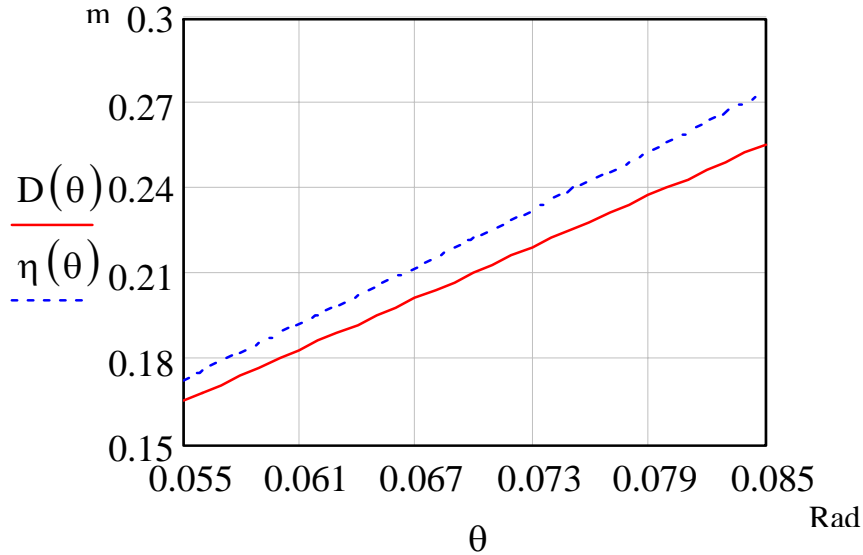


Figure 7: Maximum transverse displacement and dispersion in BC1 as functions of the bending angle.

In the ipothesis of a fixed large vacuum chamber, its horizontal gap is determined by the difference between the maximum and the minimum displacement, with the addition of the chromatic beam size (3x0.028 RMS relative energy spread x dispersion at its maximum for the left side and at its minimum for the right side) and of the trajectory error of 1 mm:

$$D_{\min}(\theta_{\min}) = 0.16515 \text{ m} \quad D_{\max}(\theta_{\max}) = 0.25554 \text{ m}$$

$$\eta_{\max}(\theta_{\max}) = 0.27354 \text{ m} \quad \eta_{\min}(\theta_{\min}) = 0.17268 \text{ m}$$

$$\text{left_margin} = 0.02298 \text{ m} \quad \text{right_margin} = 0.01451 \text{ m}$$

Thus, the total horizontal gap for the fixed vacuum chamber at the centre of the chicane is:

$$\text{fixed horizontal gap} = 13.0 \text{ cm}$$

In the ipothesis of a movable vacuum chamber, one can ignore the transverse displacement, since the chamber will follow the variation of the bending angle. In this case the total gap is defined by the maximum chromatic beam size in correspondence of the maximum RMS relative energy spread and of the maximum dispersion, with the addition of the trajectory error of 1 mm:

$$\text{movable horizontal gap} = 5.0 \text{ cm}$$

Notice that in this case the centre of mass of the electron beam, which will be detected by the Beam Position Monitor (BPM), will be always centered in the vacuum chamber with an uncertainty only due to the trajectory error (estimated in $\pm 500 \mu\text{m}$).

3. Compression in BC2

3.1 Acceleration

The compression in the second chicane is prepared through the upstream L2 and L3, which add their energy chirp to that of L1. The average beam energy and the linear energy chirp at BC2 are (for $i = 1, 2, 3$):

$$E_f(\phi_1) := U_0 + U_1 \cdot \cos(\phi_1) + U_4 \cos(\phi_4) + U_2 \cos(\phi_{2.0}) + U_3 \cos(\phi_{3.0})$$

$$h(\phi_1) := \frac{-k \sum_i U_i \sin(\phi_i) + \frac{1}{4} \cdot k \cdot [U_0 + (\sum_i U_i \cdot \cos(\phi_i))] \cdot \tan(\phi_4)}{E_f(\phi_1)}$$

RMS relative energy spread at BC2 never exceeds 1.3% (simulations result), where the upstream L2 and L3 are set to the off-crest phase of -20 deg in the extreme case (medium bunch). Like for BC1, the RMS absolute energy spread has been fixed to 6 MeV (conservative value). Under this assumptions and fixing the nominal phases for L2 and L3 at -20 deg, the beam average energy and the RMS relative energy spread at BC2 have been plotted in Figure 8 and Figure 9, respectively.

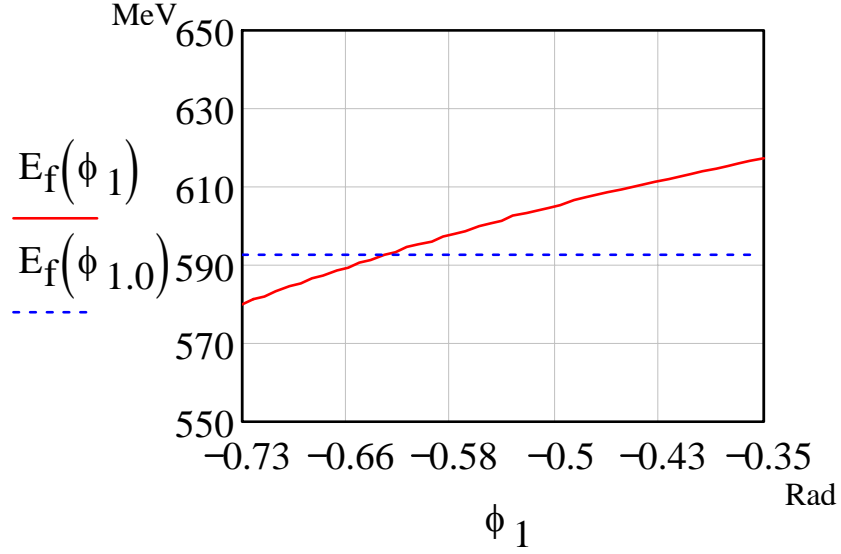


Figure 8: average beam energy at BC2 as function of the L1 phase (red line). The dashed line shows the nominal energy for the medium bunch case.

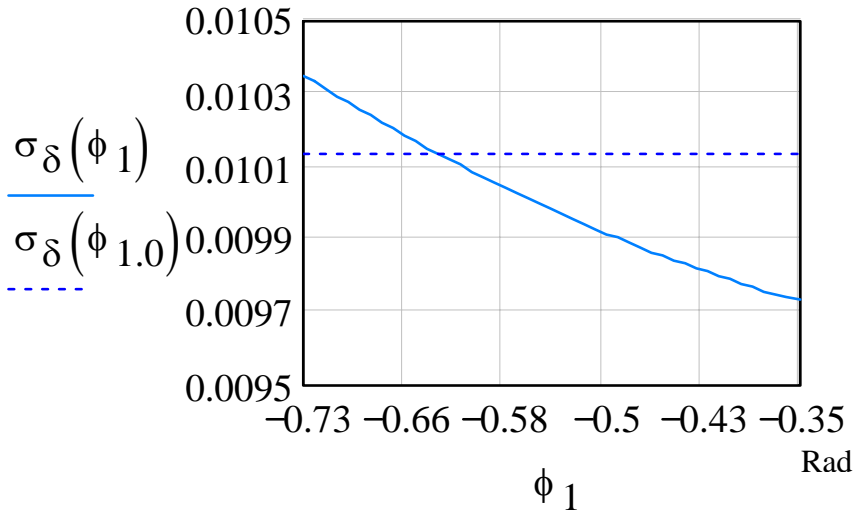


Figure 9: RMS relative energy spread at BC2 as function of the L1 phase (red line). The dashed line is the nominal value for the medium bunch case.

3.2 Compression factor

The second magnetic chicane has been studied with a bending angle in the range:

$$0.0531 \text{ rad} < \theta_b < 0.0775 \text{ rad}$$

which covers all the three scenarios regarding the final electron beam. Figure 10 shows the R_{56} term as function of the bending angle in the range just defined.

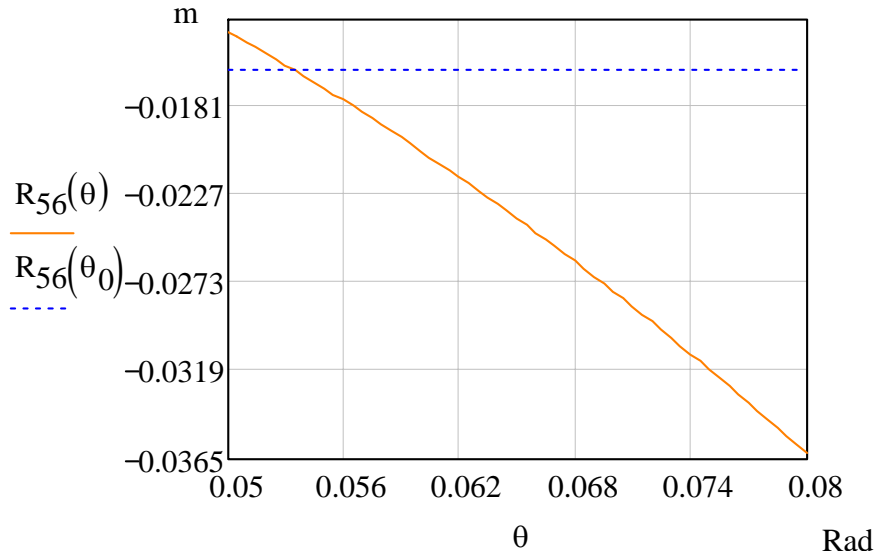
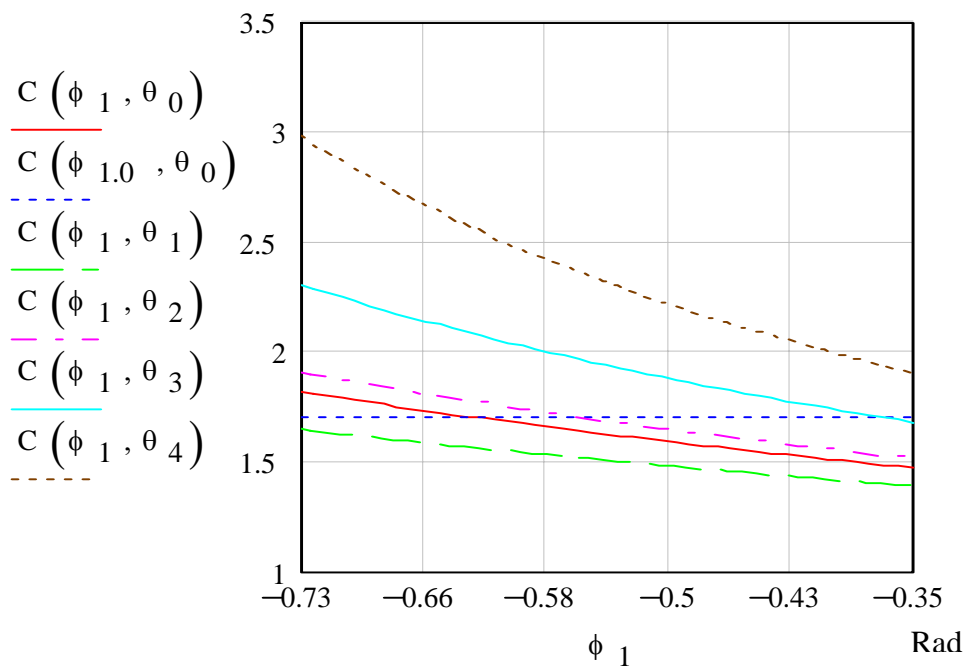


Figure 10: R_{56} term of the linear transport matrix of BC2 as function of the bending angle θ_b (solid line). The dashed line is the nominal value for the medium bunch case.

The compression factor at BC2 has been plotted in Figure 11 and Figure 12 as function of the L1 phase for several discrete values of the bending angle in the chicane, reported in Table 5. In this case the L2 and L3 phases are fixed to -20 deg (values for the nominal operation of the chicane).

Table 5: bending angle in BC2

	θ_0	θ_1	θ_2	θ_3	θ_4	θ_5	θ_6	θ_7
Bending angle [rad]	0.0535	0.050	0.055	0.060	0.065	0.070	0.075	0.080



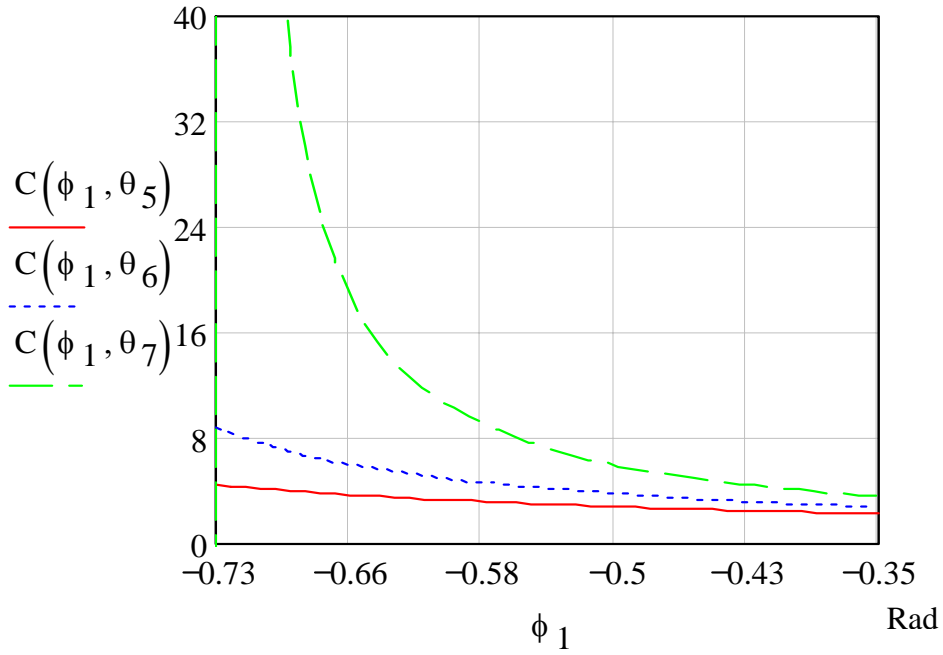


Figure 11 (upper) and Figure 12 (lower): compression factor in BC2 as function of the upstream L1 phase; each curve refers to a parametric value of the bending angle, as listed in table 5. The red line in Figure 11 is the compression factor as function of the L1 phase for the nominal bending angle of the medium bunch case; since the long bunch has a similar L1 phase (see, Table 3), the same curves may applied to this case. The blue dashed line is the compression factor for both the nominal bending angle and L1 phase for the medium bunch case. Figure 12 shows a curve which reaches the maximum compression for the bigger bending angle in Table 5.

Figure 11 and 12 demonstrate that a compression factor in BC2 between 1.5 and larger than 20 may be achieved with a bending angle within the range:

$$0.052 \text{ rad} < \theta_b < 0.080 \text{ rad}$$

3.3 Transverse displacement of the beam centroid and vacuum chamber

The same estimation like in Section 2.5 for the maximum dispersion and the maximum beam transverse displacement at the centre of BC2 has been performed; they are plotted as function of the bending angle in Figure 13. Their extreme values allow to define the horizontal gap of the vacuum chamber at that location. RMS relative energy spread of 1.5% has been taken into account in the chromatic beam size (conservative value, see Figure 9).

$$D_{\min}(\theta_{\min}) = 0.15612 \text{ m} \quad D_{\max}(\theta_{\max}) = 0.24045 \text{ m}$$

$$\eta_{\max}(\theta_{\max}) = 0.25639 \text{ m} \quad \eta_{\min}(\theta_{\min}) = 0.16286 \text{ m}$$

$$\text{left_margin} = 0.01154 \text{ m} \quad \text{right_margin} = 0.00733 \text{ m}$$

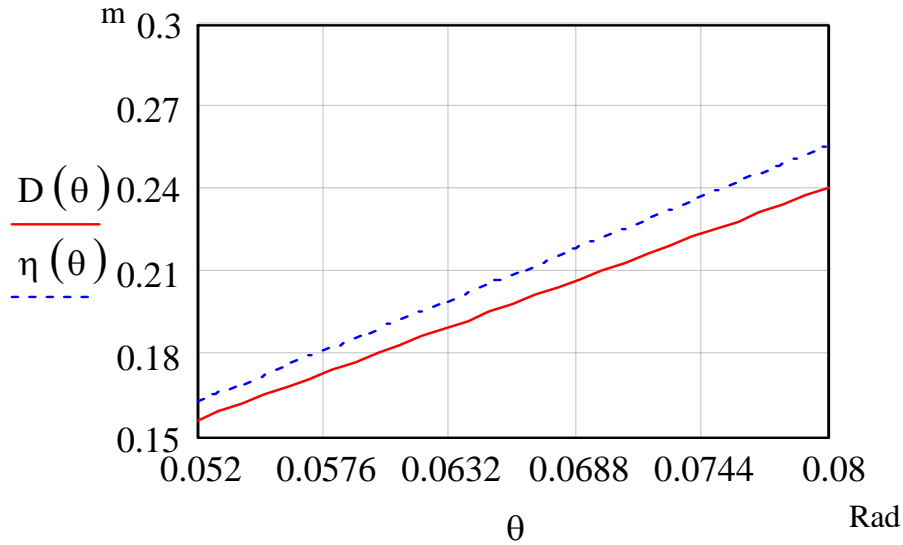


Figure 13: Maximum transverse displacement and dispersion in BC1 as functions of the bending angle.

Depending on the choice of a fixed and large vacuum chamber or one movable and smaller, the total gap results to be:

$$\text{fixed horizontal gap} = 10.6 \text{ cm}$$

$$\text{movable horizontal gap} = 2.6 \text{ cm}$$

4. Appendix: single compression scheme

The single compression scheme using only BC1 has been studied as for the short and the medium bunch cases. The short bunch option requires the strongest constraint on the bunch compression, according to the following parameters:

$$L1 \text{ phase} = -36 \text{ deg}$$

$$\theta_b = 0.0797 \text{ rad}$$

$$R_{56} = -36.0 \text{ mm}$$

$$\text{Compression factor} \geq 20$$

These values are within the range of operation already defined for BC1 in Section 2.4; thus, the short bunch option in single compression does not require any additional change to study above.

5. Conclusions

Dynamics of bunch compression in BC1 and BC2 has been described in the linear approximation. The compression factor, the dispersion function at the centre of the

chicane, the beam size including the chromatic contribution and the transverse displacement of the beam centroid at that location have been calculated and plotted as function of the bending angle and of the L1 phase. The nominal range of operation of the two chicanes has been summarized for all the three scenarios regarding the final electron bunch, that is Short, Medium and Long bunch in a double compression scheme. A possible range of operation for the machine commissioning and further studies and for the machine optimization has been suggested. As a consequence, the horizontal width of the vacuum chamber in the chicanes has been calculated, including safety margins; two options have been considered, a fixed and a movable vacuum chamber, respectively.

As for BC1, the range of operation of the bending angle (per dipole) has been decided in:

$$0.055 \text{ rad} < \theta_b < 0.085 \text{ rad}$$

It is associated to an off-crest acceleration of the L1 with phase within:

$$- 42 \text{ deg} < \phi_1 < - 20 \text{ deg}$$

The resulting horizontal dispersion is within the range $0.170 \text{ m} < \eta_x < 0.275 \text{ m}$, while the transverse displacement of the bunch centroid w.r.t the straight path is within the range $0.165 \text{ m} < D_x < 0.260 \text{ m}$.

Consequently, the total width of the vacuum chamber is 13.0 cm for the fixed option and 5.0 cm for the movable one.

As for BC2, the range of operation of the bending angle (per dipole) has been decided in:

$$0.052 \text{ rad} < \theta_b < 0.080 \text{ rad}$$

It is associated to the same off-crest acceleration of the L1 as said above, while the L2 and L3 phase move within the range:

$$- 30 \text{ deg} < \phi_{2,3} < 0 \text{ deg}$$

The resulting horizontal dispersion is within the range $0.160 \text{ m} < \eta_x < 0.260 \text{ m}$, while the transverse displacement of the bunch centroid w.r.t the straight path is within the range $0.155 \text{ m} < D_x < 0.240 \text{ m}$.

Consequently, the total width of the vacuum chamber is 10.6 cm for the fixed option and 2.6 cm for the movable one.

Acknowledgement

The author thanks Marco Veronese and Mario Ferianis for the useful and clarifying discussions on the chicanes geometry and associated diagnostics.